In Vivo Characterization of Proliferation for Discriminating Cancer from Pancreatic Pseudotumors

Ken Herrmann*[1], Florian Eckel*[2], Stefan Schmidt[3], Klemens Scheidhauer[1], Bernd Joachim Krause[1], Joerg Kleeff[4], Tibor Schuster[5], Hans-Juergen Wester[1], Helmut Friess[4], Roland M. Schmid[2], Markus Schwaiger[1], and Andreas K. Buck[1]

[1]Department of Nuclear Medicine, Technische Universität München, Munich, Germany; [2]Department of Internal Medicine II, Technische Universität München, Munich, Germany; [3]Department of Radiology, Technische Universität München, Munich, Germany; [4]Department of Surgery, Technische Universität München, Munich, Germany; and [5]Department of Medical Statistics, Technische Universität München, Munich, Germany

We have determined the ability of PET with the thymidine analog 3′-deoxy-3′-^{18}F-fluorothymidine (FLT) to detect pancreatic cancer and to differentiate malignant from benign pancreatic lesions. **Methods:** In this prospective study, ^{18}F-FLT PET was performed on 31 patients with undefined pancreatic lesions. Routine diagnostic procedures included endoscopic ultrasound, MRI, or multislice helical CT of the upper gastrointestinal tract in all patients. Uptake of ^{18}F-FLT was evaluated semiquantitatively by calculation of mean and maximal standardized uptake values (SUVs). Results were correlated to the reference methods, which were histopathology (23/31) or cytology/clinical follow-up (8/31). **Results:** All 10 benign pancreatic lesions were negative on ^{18}F-FLT PET and showed only background activity (specificity, 100%; 90% confidence interval, 74%−100%). On visual interpretation, 15 of 21 malignant tumors presented as focal ^{18}F-FLT uptake higher than the surrounding background (sensitivity, 71.4%; 90% confidence interval, 52%−89%). ^{18}F-FLT PET missed 4 well-differentiated and 2 T1 cancers. Mean ^{18}F-FLT uptake was 3.1 in all malignant tumors (median, 2.8; range, 1.3–8.5), 3.7 in tumors with visual tracer uptake (median, 3.2; range, 2.1–8.5), and significantly higher in malignant than in benign tumors (mean/median, 1.4; range, 1.2–1.7; $P < 0.001$). For discriminating cancer from benign pancreatic lesions, receiver-operating-characteristic analysis indicated a sensitivity of 81% and specificity of 100% (area under the curve, 0.93) using a mean ^{18}F-FLT SUV cutoff of 1.8 (maximal ^{18}F-FLT SUV: area under the curve, 0.92; SUV cutoff, 2.1). **Conclusion:** In this pilot study, focal uptake of the in vivo proliferation marker ^{18}F-FLT was detected exclusively in malignant tumors. ^{18}F-FLT PET may therefore be useful as a diagnostic adjunct for differentiating cancer from benign pancreatic lesions.

Key Words: nucleoside analogs; pancreatic tumors; differential diagnosis; proliferation; positron emission tomography

J Nucl Med 2008; 49:1437–1444
DOI: 10.2967/jnumed.108.052027

Chronic pancreatitis (CP) is considered one of the risk factors for the development of pancreatic ductal adenocarcinoma. Differentiating between pseudotumoral masses resulting from CP and pancreatic carcinoma can be clinically challenging because the two have similar imaging features and clinical presentations. To date, no single diagnostic approach is considered ideal for differentiating between pancreatic cancer and pseudotumoral CP (*1*). Several overlapping morphologic features of CP and pancreatic carcinoma contribute to and explain the limitations in differential diagnosis (*2*). CT examination is limited in identifying the ductal adenocarcinoma that begins during CP because of the reduced difference in density between the cancerous lesion, which is typically hypovascularized, and the pancreatic parenchyma, which is also typically hypovascularized in CP because of fibrosis (*3*). Up to 6% of the cases suspected to be malignant have been found to be benign at surgery, which may be associated with a postsurgical complication rate of up to 21% (*4*). Endoscopic ultrasound (EUS) has become the most accurate modality for the characterization, locoregional staging, and sampling of pancreatic lesions. EUS-guided fine-needle aspiration of suggestive tumors significantly improves the diagnostic reliability of EUS and should be regarded as the first choice for diagnosis in this setting. However, the improved sensitivity of EUS-guided fine-needle aspiration was only 73% in 1 trial (*1*), indicating that the diagnosis of evolving carcinoma in the background of CP remains difficult.

PET with the glucose analog ^{18}F-FDG is highly sensitive for detecting pancreatic cancer. However, ^{18}F-FDG also accumulates in inflammatory lesions (*5*). Therefore, dis-

Received Apr. 26, 2008; revision accepted May 5, 2008.
For correspondence or reprints contact: Andreas K. Buck, Department of Nuclear Medicine, Technische Universität München, Ismaninger Strasse 22, D-81675 Munich, Germany
E-mail: andreas.buck@tum.de
*Contributed equally to this work.

crimination of benign from malignant pancreatic masses with ^{18}F-FDG PET is problematic. The thymidine analog 3′-deoxy-3′-^{18}F-fluorothymidine (FLT) is a new radiopharmaceutical for clinical PET that specifically visualizes proliferating tissues (*6,7*). In the present study, we aimed to determine whether ^{18}F-FLT PET is adequate for detection of pancreatic cancer and differentiation of cancer from benign pancreatic lesions such as mass-forming pancreatitis.

MATERIALS AND METHODS

Patient Population

Thirty-one patients with a clinical suspicion of malignant pancreatic disease were included in this prospective study (22 men and 9 women; mean age, 61 ± 13 y; range, 39–79 y). Patients were recruited in the outpatient clinic of the Department of Internal Medicine II (gastroenterology) or the Department of General Surgery at Technische Universität München. Most patients were referred to our hospital for a further diagnostic work-up because of a new onset of jaundice or pain in the upper abdomen. Inclusion criteria comprised an initial diagnosis of a suggestive pancreatic tumor, diagnosed either by ultrasound, EUS, MRI, multislice helical CT, endoscopic retrograde cholangiopancreatography, or a combination of these. Patients with a history of CP and a new onset of extrahepatic biliary obstruction or increasing tumor markers CA 19–9 or CEA were also included.

Staging procedures included abdominal ultrasound, endoscopic retrograde cholangiopancreatography, EUS, MRI, or multislice CT of the chest and abdomen as clinically appropriate. Histologic or cytologic confirmation was obtained in most patients (23/31 and 5/31 patients, respectively). In cases of negative histologic or cytologic findings, EUS-guided fine-needle aspiration and biopsy or brushing of the distal bile duct was performed during follow-up. Informed consent was obtained from all patients. The study protocol was approved by the local ethics committee of Technische Universität München.

^{18}F-FLT PET

^{18}F-FLT was synthesized as previously described (*8*). Imaging was performed on a whole-body PET scanner (ECAT HR+; Siemens/CTI). This scanner simultaneously acquires 47 contiguous slices with a slice thickness of 3.4 mm. The in-plane image resolution of transaxial images was approximately 8 mm in full width at half maximum, with an axial resolution of approximately 5 mm in full width at half maximum. Static emission images were acquired 45 min after injection of approximately 300 MBq of ^{18}F-FLT (range, 270–340 MBq). ^{18}F-FLT PET was performed from the thorax to the pelvis (4–5 bed positions) for all patients. The duration was 8 min per bed position for emission scanning and 5 min for transmission scanning. Emission data were corrected for random coincidences, dead time, and attenuation and were reconstructed by filtered backprojection (Hanning filter with a cutoff frequency of 0.4 cycles per bin). The matrix size was 128 × 128 pixels, with a pixel size of 4.0 × 4.0 mm. The image pixel counts were calibrated to activity concentrations (Bq/mL) and decay-corrected using the time of tracer injection as the reference.

PET Data Analysis

All ^{18}F-FLT PET scans were evaluated by 2 experienced nuclear medicine physicians who were unaware of the clinical data and the results of other imaging studies. Any focally increased ^{18}F-FLT uptake in the upper abdomen was interpreted as malignant. Side-by-side reading with a recent multislice CT scan of the abdomen was performed to ensure that increased ^{18}F-FLT uptake belonged to pancreatic tissue. When results between the 2 readers differed, they reached a consensus.

Circular regions of interest with a diameter of 1.5 cm were placed in the area with the highest tumor activity as described earlier (*9*). Mean and maximal standardized uptake values (SUVs) were calculated from each region of interest using the following formula: SUV = measured activity concentration (Bq/g) × body weight (g)/injected activity (Bq). For definition of regions of interest and data analysis, computer programs have been developed in the Interactive Data Language (IDL; Research Systems, Inc.) using the Clinical Application Programming Package (CAPP; Siemens/CTI) (*10*).

Reference Methods for Assessment of Malignancy

In most patients (19/21), histopathology served as the reference for malignancy. Two cancer patients had the typical imaging findings of a pancreatic mass and liver metastases, indirectly demonstrating malignancy of the pancreatic tumor (patients 1 and 30). In patients from whom no specimen could be obtained, the diagnosis of CP was based on a combination of imaging methods such as multislice CT, EUS, and endoscopic retrograde cholangiopancreatography, which were repeated in due course. After patient recruitment began in April 2006, no malignant pancreatic tumor was diagnosed in patients with CP.

Statistical Analysis

Statistical analyses were performed using SPSS software (version 15.0; SPSS, Inc.). Quantitative values were expressed as mean ± SD, median, and range. Related metric measurements were compared using the Wilcoxon signed rank test and the Mann–Whitney *U* test in cases of 2 independent samples. Fisher exact tests were used for comparison of frequencies, and Spearman correlation coefficients were calculated to quantify bivariate correlations of measurement data. Exact 90% confidence intervals were reported for estimates of sensitivity and specificity. Receiver-operating-characteristic analysis was performed using SPSS software. All analyses were 2-sided and were performed at a 5% level of significance.

RESULTS

Patients with Malignant Pancreatic Lesions

Twenty-one of the 31 patients turned out to have pancreatic cancer (Fig. 1). Detailed tumor characteristics are listed in Table 1. Malignancy of the pancreatic tumor was confirmed histologically in 19 patients. In 1 patient, MRI and contrast-enhanced CT showed a typical finding of multiple liver metastases. Consequently, histologic verification of the pancreatic tumor was not performed. The second patient refused to have surgery or biopsy of the pancreatic tumor; however, the clinical course (rising level of tumor marker CA 19–9 and new onset of liver lesions on MRI and multislice CT) indicated malignant pancreatic disease. The histologic subtypes were adenocarcinoma (n = 15), cystadenocarcinoma (n = 1), squamous cell carcinoma (n = 1), neuroendocrine

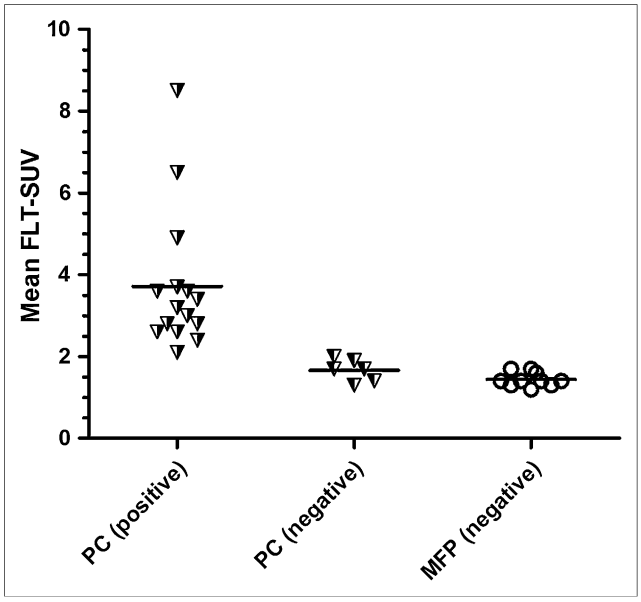

FIGURE 1. Scatter plot of mean ^{18}F-FLT SUV in pancreatic cancer with focal ^{18}F-FLT uptake (PET-positive), in pancreatic cancer negative on visual interpretation (PET-negative), and in benign pancreatic lesions (PET-negative). MFP = mass-forming pancreatitis; PC = pancreatic cancer.

carcinoma ($n = 1$), and undifferentiated carcinoma ($n = 1$). Fifteen tumors were in the head of the pancreas, 4 in the pancreatic corpus, and 2 in the tail of the pancreas (Table 1). Eight patients underwent complete surgical resection of the primary tumor. Seven patients had liver metastases, which were unresectable in 4 because of locally advanced disease. Of the latter, 1 patient died from thromboembolic complications during follow-up. In this patient, postmortem evaluation revealed stage 2b disease (American Joint Committee on Cancer staging system).

Patients with Inflammatory Lesions

Of 10 patients in whom the reference methods indicated benign disease (Fig. 1), 4 underwent surgical bypass or resection, and the benign nature of the pancreatic mass was proven histologically (Table 1). In a further 5 patients with pancreatic masses, biopsies of the pancreas, distal bile duct, or duodenum failed to demonstrate malignant disease. EUS or endoscopic retrograde cholangiopancreatography was performed in 7 and 5 patients, respectively, and was repeated at least once to exclude false-negative results in 5 and 4 patients, respectively. To date, there has been no evidence of malignant disease in this patient subgroup.

Imaging Malignant Pancreatic Tumors with ^{18}F-FLT PET

^{18}F-FLT PET produced high-contrast images of proliferating structures (Fig. 2). Fifteen of 21 patients with malignant tumors presented with focal ^{18}F-FLT uptake higher than surrounding background activity (sensitivity of ^{18}F-FLT PET, 71.4%; confidence interval, 52%−89%). By visual interpretation, 6 tumors did not show focally increased tracer uptake, compared with the surrounding normal background activity (Tables 1–3; Fig. 3). The mean ^{18}F-FLT uptake in all malignant tumors was 3.1 (median, 2.8; range, 1.3–8.5; SD, 1.7). In PET-positive tumors, the mean ^{18}F-FLT uptake was 3.7 (median, 3.2; range, 2.1–8.5), being significantly higher than in PET-negative tumors (mean/median, 1.4; range, 1.2–1.7; $P = 0.001$) (Figs. 2 and 3; Table 2). The average maximal ^{18}F-FLT uptake in all malignant tumors was 3.7 (median, 3.5; range, 1.5–9.8). Mean maximal ^{18}F-FLT uptake was significantly higher in PET-positive tumors (4.4; median, 4.2; range, 2.6–9.8) than in PET-negative tumors (mean/median, 1.7; range, 1.5–2.0; $P = 0.001$).

The histology of the 6 pancreatic cancers negative on ^{18}F-FLT PET differed considerably from the ^{18}F-FLT–positive tumors. Most of the ^{18}F-FLT–negative tumors did not consist of the typical aggressive ductal subtype. There was 1 cystic adenocarcinoma, 2 tubular adenocarcinomas, and 1 poorly differentiated carcinoma not further classified. Most of these were of low tumor grade (1 grade I, 1 grade I–II, and 1 grade II). Furthermore, 2 of the ^{18}F-FLT–negative cancers were small tumors (clinical stage T1 with a size < 20 mm on multislice CT or MRI).

Seven patients presented with liver metastases as indicated by MRI (3 patients) or helical CT (4 patients). One patient also had histologic verification of liver metastases. In 6 of these, ^{18}F-FLT showed reduced or absence of tracer uptake in corresponding lesions, compared with surrounding normal tissue. In another patient, metastatic sites presented as increased focal tracer uptake in the tumor margin, with a photopenic defect in the center of the lesion.

Imaging Benign Pancreatic Lesions with ^{18}F-FLT PET

All 10 patients in whom the reference methods indicated benign disease presented without focal tracer uptake (specificity, 100%; confidence interval, 74%−100%) (Tables 2 and 3). Mean ^{18}F-FLT SUV in benign pancreatic lesions was 1.4 (median, 1.4; range, 1.2–1.7), being similar to background activity and significantly lower than in malignant lesions ($P < 0.001$). The mean maximal ^{18}F-FLT uptake in all benign lesions was also significantly lower than in malignant lesions (mean/median, 1.7/1.6; range, 1.5–2.0; $P < 0.001$) (Fig. 2).

Discriminating Cancer from Benign Pancreatic Lesions Using ^{18}F-FLT PET

Using visual interpretation criteria (focally increased ^{18}F-FLT uptake, compared with surrounding normal structures), the sensitivity, specificity, and accuracy of ^{18}F-FLT PET were 71.4% (15/21), 100% (10/10), and 81% (25/31), respectively. Receiver-operating-characteristic analysis (Fig. 4) indicated a sensitivity of 81%, a specificity of 100%, and an accuracy of 87%, with an area under the curve of 0.929 using a cutoff of 1.8 for mean ^{18}F-FLT SUV. Using maximal ^{18}F-FLT SUV, the same values (81%, 100%, and 87%) were calculated using a cutoff level of 2.1 for maximal ^{18}F-FLT SUV, with an area under the curve of 0.919.

TABLE 1
Tumor Characteristics, Lesion Location, ^{18}F-FLT PET Findings, Reference Method, and Clinical Consensus

Patient no.	Lesion location	^{18}F-FLT mean SUV	^{18}F-FLT maximal SUV	^{18}F-FLT PET visual score	Reference method	Clinical consensus
1	Head	3.6	4.2	1	Met, CFU	1
2	Head	1.2	1.5	0	Benign pancreatic tissue (C), CFU	0
3	Tail	3.2	3.5	1	Adenocarcinoma (H)	1
4	Head	1.6	1.8	0	Benign pancreatic tissue (C), CFU	0
5	Head	3.7	4.4	1	Adenocarcinoma (H)	1
6	Tail	2.8	3.5	1	Adenocarcinoma (H)	1
7	Head	1.7	2.0	0	Benign pancreatic tissue (H)	0
8	Head/corpus	1.4	1.7	0	Benign pancreatic tissue (H)	0
9	Head	1.4	1.6	0	Benign pancreatic tissue (C), CFU	0
10	Head	6.5	7.3	1	Squamous cell carcinoma (H)	1
11	Head	2.6	3.1	1	Adenocarcinoma (H)	1
12	Head	8.5	9.8	1	Undifferentiated adenocarcinoma (H)	1
13	Head	1.3	1.6	0	Benign pancreatic tissue (H)	0
14	Head	2.4	2.6	1	Neuroendocrine carcinoma (H)	1
15	Head	2.8	3.8	1	Adenocarcinoma (H)	1
16	Corpus	1.7	2.0	0	Adenocarcinoma (H)	1
17	Head	2.0	2.2	0	Cystadenocarcinoma (H)	1
18	Head	1.3	1.5	0	Adenocarcinoma (H)	1
19	Head	3.4	3.9	1	Adenocarcinoma (H)	1
20	Corpus	1.9	2.3	0	Adenocarcinoma (H)	1
21	Corpus	1.3	1.5	0	CFU	0
22	Head	1.4	1.6	0	Benign pancreatic tissue (H)	0
23	Head	4.9	5.1	1	Adenocarcinoma (H)	1
24	Head	1.7	1.9	0	Benign pancreatic tissue (C), CFU	0
25	Head	1.4	1.6	0	Benign pancreatic tissue (C), CFU	0
26	Corpus	2.6	3.0	1	Adenocarcinoma (H)	1
27	Head	3.0	3.4	1	Adenocarcinoma (H)	1
28	Head	2.1	4.1	1	Adenocarcinoma (H)	1
29	Head	1.7	1.9	0	Adenocarcinoma (H)	1
30	Corpus	1.4	1.6	0	Met, CFU	1
31	Head	3.6	4.2	1	Adenocarcinoma (H)	1

0 = benign; 1 = malignant; met = liver mets at MRI/CT; CFU = clinical follow-up; C = cytology; H = histology.

Nineteen of 21 malignant and 4 of 10 benign lesions were verified histologically. Cytology or clinical follow-up served as reference in remaining patients.

DISCUSSION

Recently, the thymidine analog ^{18}F-FLT was suggested for noninvasive assessment of proliferation (*11*). In this pilot study, we demonstrated that PET with the in vivo proliferation marker ^{18}F-FLT is specific for malignant pancreatic tumors and may be used to noninvasively differentiate pancreatic cancer from pancreatic pseudotumors arising from CP. In our patient collective, all lesions that turned out to be of benign origin were negative on ^{18}F-FLT PET. Fifteen of 21 malignant tumors presented as focally increased tracer uptake, indicating a sensitivity of 71.4% for detecting malignant disease. Using a threshold of 1.8 for mean ^{18}F-FLT SUV, we found that sensitivity increased to 81% (maximal ^{18}F-FLT SUV, 2.1) and receiver-operating-characteristic analysis indicated an area under the curve of 0.93. Frequently, differential diagnosis of pancreatic tumors is challenging. Because of the high specificity, positive PET findings indicate cancer of the pancreas. ^{18}F-FLT PET may therefore aid in the decision-making process by further ensuring the appropriateness of resective surgery.

When scan findings are negative, cancer cannot be excluded. ^{18}F-FLT–negative tumors turned out to differ significantly from PET-positive tumors regarding histologic subtype, tumor size, tumor grade, and clinical course. There were 2 T1 cancers, indicating a reduced sensitivity of ^{18}F-FLT PET for detecting small primaries. A reduced sensitivity for small pancreatic cancers has also been described for the standard radiotracer ^{18}F-FDG, presumably because of partial-volume effects (*12*). Moreover, tumor grade was low in most ^{18}F-FLT–negative tumors, and survival of these patients was favorable. Although a definite conclusion regarding a potential clinical role cannot yet be drawn, our pilot study suggests prognostic potential for ^{18}F-FLT PET and warrants evaluation in a larger series.

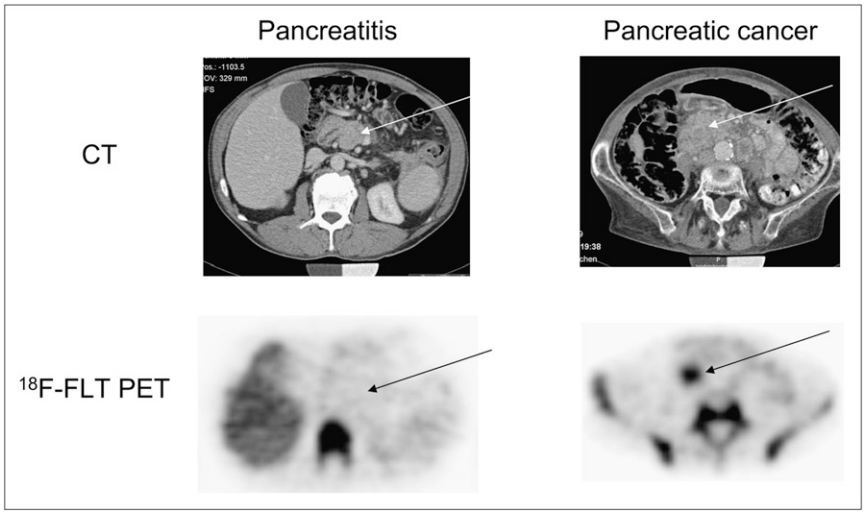

FIGURE 2. Spiral CT and ^{18}F-FLT PET of patient 21, with CP, and patient 23, with pancreatic cancer. Physiologically increased ^{18}F-FLT uptake is seen in bone marrow and liver, but only background activity of ^{18}F-FLT is seen in area of inflammatory pancreatic mass (true-negative). Focal ^{18}F-FLT uptake is seen in pancreatic carcinoma (true-positive).

With morphology-based imaging modalities such as CT, MRI, or EUS, differentiation of benign pancreatic tumors associated with CP and pancreatic adenocarcinoma remains problematic because of similar anatomic features. EUS has become the standard modality for the characterization of pancreatic tumors and locoregional staging of pancreatic cancer. EUS-guided fine-needle aspiration further improves the diagnostic reliability of EUS (*1*); however, because of sampling errors, diagnosis of early cancers arising from mass-forming pancreatitis remains difficult. A positive or negative ^{18}F-FLT PET scan may aid in the decision process if the clinical suspicion of pancreatic cancer is high and patients are potential candidates for surgical resection.

In principle, having a functional imaging test to complement standard diagnostic modalities would be advantageous. ^{18}F-FDG PET is now an accepted technology for differential diagnosis and staging of various cancers (*13*). In pancreatic cancer, ^{18}F-FDG PET has also been shown to be more accurate than other modalities but less specific when acute inflammation is present (*14–16*). Expression of the glucose transporter-1 gene and membrane glucose transport is generally increased in pancreatic cancer but not in CP (*17*). In contrast, it has been shown that inflammatory cells such as neutrophils or activated macrophages avidly take up ^{18}F-FDG (*18,19*). Accordingly, ^{18}F-FDG has been reported to accumulate in various inflammatory processes (*20,21*), including acute pancreatitis (*12*). Therefore, Diederichs et al. (*14*) recommended excluding patients with evidence of acute-on-chronic pancreatitis by laboratory data to minimize false-positive PET findings. ^{18}F-FDG PET is also affected by other metabolic conditions such as altered glucose metabolism, causing a decreased sensitivity for detection of pancreatic cancer in patients with elevated plasma glucose levels (*22,23*).

^{18}F-FDG PET may also be inferior to MRI or spiral CT for detecting pancreatic cancer but is more accurate for detecting distant metastases (*24–27*). In a study by Heinrich et al., the sensitivity of combined ^{18}F-FDG PET/CT for detecting locoregional lymph node metastases was as low as 22%. However, in 5 of 59 patients with pancreatic

TABLE 2
^{18}F-FLT PET Findings, Using Visual Interpretation, Compared with Clinical Consensus

	Clinical consensus		
^{18}F-FLT PET finding	Pancreatic cancer	Benign pancreatic lesion	Total
Negative	6	10	16
Positive	15	0	15
Total	21	10	31

Clinical consensus is based on histologic verification in 23 patients, clinical follow-up/cytologic analysis in 7 patients, and evidence of metastatic disease on CT and MRI in 1 patient. Sensitivity of ^{18}F-FLT PET is 71%; specificity, 100%.

TABLE 3
^{18}F-FLT PET Findings, Using Cutoff of 1.8 for Mean SUV or 2.1 for Maximal SUV, Compared with Clinical Consensus

	Clinical consensus		
^{18}F-FLT PET finding	Pancreatic cancer	Benign pancreatic lesion	Total
Negative	4	10	14
Positive	17	0	17
Total	21	10	31

Clinical consensus is based on histologic verification in 23 patients, clinical follow-up/cytologic analysis in 7 patients, and evidence of metastatic disease on CT and MRI in 1 patient. Sensitivity of ^{18}F-FLT PET is 81%; specificity, 100%.

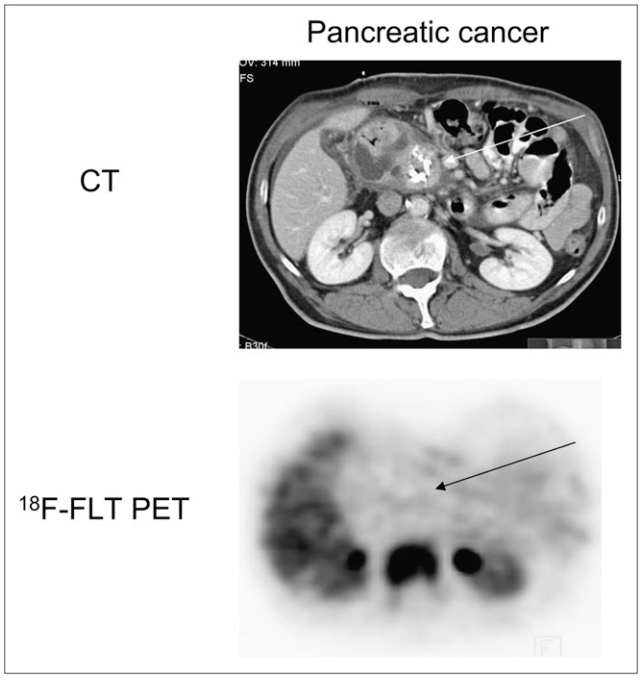

FIGURE 3. Spiral CT and ^{18}F-FLT PET of patient 18, with pancreatic cancer, and false-negative findings on ^{18}F-FLT PET. Physiologic ^{18}F-FLT uptake is seen in bone marrow and liver. Histology indicated T1 adenocarcinoma.

cancer, previously unknown distant metastases were detected with ^{18}F-FDG PET/CT and surgery was avoided. This has led to a cost reduction of $63,000, indicating that the use of ^{18}F-FDG PET/CT may be cost-efficient despite the mentioned shortcomings (*24*). Even in the presence of inflammatory disease, ^{18}F-FDG PET may be helpful in detecting pancreatic cancer in patients with CP (*27*). However, the patient numbers are small, and the clinical role of PET for managing undefined pancreatic tumors or staging pancreatic cancer remains to be determined.

The use of integrated PET/CT scanners has been suggested for increasing the accuracy of PET. However, in 1 study, the sensitivity of PET/CT for detecting locoregional lymph node involvement was low whereas the sensitivity for distant metastases was acceptable (88%) (*24*). Specific imaging of proliferation using ^{18}F-FLT may overcome some of the limitations associated with ^{18}F-FDG. In a previous study, we demonstrated that ^{18}F-FDG uptake is similarly increased in CP and pancreatic adenocarcinoma. In contrast, tumor proliferation as determined by immunohistochemistry could better differentiate between benign and malignant pancreatic tumors than could altered glucose metabolism (*5*). The mean percentage of Ki-67–positive cells was about 10-fold higher in pancreatic cancer than in CP, indicating that proliferative activity is strongly elevated in pancreatic carcinoma but only slightly elevated in CP. For pancreatic tumors, tracers reflecting proliferative activity, such as ^{11}C-thymidine or ^{18}F-FLT (*11*), offer advantages over ^{18}F-FDG and may be more suitable for differentiating malignant from inflammatory processes. The operating expenses for synthesis of ^{18}F-FLT are similar to those for ^{18}F-FDG, further supporting its clinical application.

^{18}F-FLT turned out to be specific for pancreatic cancer; however, the major drawback of our series was a reduced sensitivity for malignant lesions. A similar reduction in sensitivity was found in a recent pilot study comprising 5 patients with pancreatic cancer (*28*) and in 2 larger series in lung cancer (*6,29*). Moreover, reduced detection rates of liver metastases have been described in colorectal cancer (*30*) and non–small cell lung cancer (*31*). In our series, liver metastases were present in 7 patients and predominantly appeared as areas of reduced tracer uptake, compared with surrounding normal tissue. Therefore, small liver metastases may also be missed in pancreatic cancer, impairing the potential of ^{18}F-FLT PET for tumor staging.

The rationale for the use of ^{18}F-FLT as a surrogate marker of cellular proliferation is based on its substrate specificity for the cell cycle–regulated protein thymidine kinase 1. Barthel et al. reported that in vivo uptake of ^{18}F-FLT is closely related to thymidine kinase 1 activity and the cellular concentration of adenosine triphosphate (*32*). However,

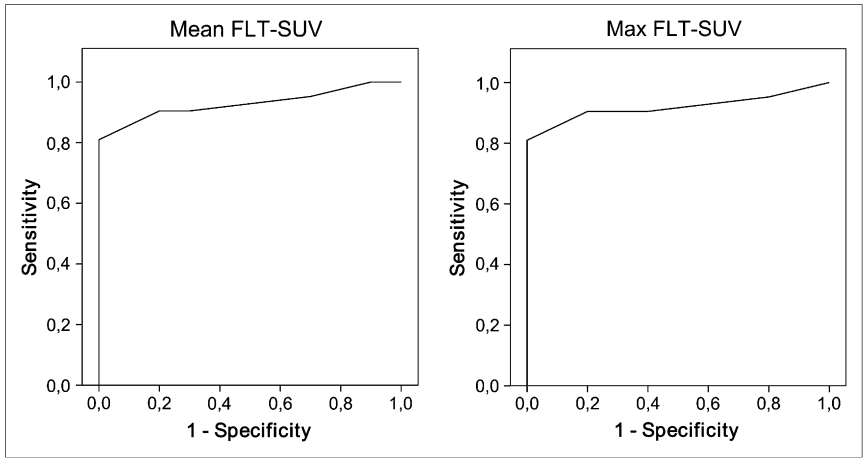

FIGURE 4. Receiver-operating-characteristic analysis of ^{18}F-FLT PET for discriminating cancer from benign pancreatic lesions. Area under curve is 0.93 using cutoff of 1.8 for mean SUV or 0.92 using cutoff of 2.1 for maximal SUV.

^{18}F-FLT acts as a chain terminator and is therefore not incorporated into DNA and represents no direct measure of proliferation (*33*). Perumal et al. showed that ^{18}F-FLT uptake is also related to the expression of nucleoside transporters (*34*). After treatment with inhibitors of thymidylate de novo synthesis such as 5-fluorouracil or methotrexate, a 7- to 10-fold increase in ^{18}F-FLT uptake was observed in esophageal carcinoma cells. This finding may be related to an activation of the thymidylate salvage pathway and a concomitant increase in thymidine kinase 1 activity (*35*). However, the detailed uptake mechanism of ^{18}F-FLT in various tumors remains to be determined, especially in pancreatic tumors.

Several limitations have to be considered when our results are transferred to the clinical situation. Our findings apply to a particular patient collective that did not cover all histologic subtypes of pancreatic tumors. Whereas most of the ^{18}F-FLT PET literature reports relatively specific uptake of ^{18}F-FLT in malignant tumors (*6,7,30,36–39*), nonspecific uptake in reactive cervical lymph nodes of patients with head and neck cancer has recently been described (*40*). An increased proliferation rate is not specific for malignant tumors, and thus, unspecific uptake of ^{18}F-FLT in reactive nodes or inflammatory pancreatic lesions cannot be excluded.

CONCLUSION

Focal uptake of the thymidine analog ^{18}F-FLT was observed exclusively in malignant pancreatic tumors, indicating a potential role in the differential diagnosis of undefined lesions. These promising results warrant analysis in a larger series that also evaluates the prognostic role of ^{18}F-FLT PET in pancreatic cancer.

ACKNOWLEDGMENTS

We appreciate the excellent contributions made by our colleagues Jens Stollfuss, Hans Höfler, Alexander Kroiss, Petra Watzlowik, Karin Kantke, and Michael Herz; the great support by Christine Praus; our students Barbara Numberger and Daniela Zwiesler; and our technical staff members Brigitte Dzewas and Coletta Kruschke. This work was supported by grant LSHC-CT-2004-503569 from EMIL (European Molecular Imaging Laboratories).

REFERENCES

1. Ardengh JC, Lopes CV, Campos AD, Pereira de Lima LF, Venco F, Modena JL. Endoscopic ultrasound and fine needle aspiration in chronic pancreatitis: differential diagnosis between pseudotumoral masses and pancreatic cancer. *JOP.* 2007;8:413–421.
2. Balthazar EJ. Pancreatitis associated with pancreatic carcinoma: preoperative diagnosis—role of CT imaging in detection and evaluation. *Pancreatology.* 2005;5:330–344.
3. Graziani R, Tapparelli M, Malago R, et al. The various imaging aspects of chronic pancreatitis. *JOP.* 2005;6(1, suppl)73–88.
4. van Gulik TM, Reeders JW, Bosma A, et al. Incidence and clinical findings of benign, inflammatory disease in patients resected for presumed pancreatic head cancer. *Gastrointest Endosc.* 1997;46:417–423.
5. Buck AC, Schirrmeister HH, Guhlmann CA, et al. Ki-67 immunostaining in pancreatic cancer and chronic active pancreatitis: does in vivo FDG uptake correlate with proliferative activity? *J Nucl Med.* 2001;42:721–725.
6. Buck AK, Halter G, Schirrmeister H, et al. Imaging proliferation in lung tumors with PET: ^{18}F-FLT versus ^{18}F-FDG. *J Nucl Med.* 2003;44:1426–1431.
7. Wagner M, Seitz U, Buck A, et al. 3′-[^{18}F]fluoro-3′-deoxythymidine ([^{18}F]-FLT) as positron emission tomography tracer for imaging proliferation in a murine B-cell lymphoma model and in the human disease. *Cancer Res.* 2003;63:2681–2687.
8. Machulla HJ, Blocher A, Kuntzsch M, Grierson JR. Simplified labeling approach for synthesizing 3′-deoxy-3′-[^{18}F]fluorothymidine ([^{18}F]FLT). *J Radioanal Nucl Chem.* 2000;24:843–846.
9. Herrmann K, Wieder HA, Buck AK, et al. Early response assessment using 3′-deoxy-3′-[^{18}F]fluorothymidine-positron emission tomography in high-grade non-Hodgkin's lymphoma. *Clin Cancer Res.* 2007;13:3552–3558.
10. Weber WA, Ziegler SI, Thodtmann R, Hanauske AR, Schwaiger M. Reproducibility of metabolic measurements in malignant tumors using FDG PET. *J Nucl Med.* 1999;40:1771–1777.
11. Shields AF, Grierson JR, Dohmen BM, et al. Imaging proliferation in vivo with [F-18]FLT and positron emission tomography. *Nat Med.* 1998;4:1334–1336.
12. Diederichs CG, Staib L, Vogel J, et al. Values and limitations of ^{18}F-fluorodeoxyglucose-positron-emission tomography with preoperative evaluation of patients with pancreatic masses. *Pancreas.* 2000;20:109–116.
13. Juweid ME, Stroobants S, Hoekstra OS, et al. Use of positron emission tomography for response assessment of lymphoma: consensus of the Imaging Subcommittee of International Harmonization Project in Lymphoma. *J Clin Oncol.* 2007;25:571–578.
14. Diederichs CG, Staib L, Glasbrenner B, et al. F-18 fluorodeoxyglucose (FDG) and C-reactive protein (CRP). *Clin Positron Imaging.* 1999;2:131–136.
15. Friess H, Langhans J, Ebert M, et al. Diagnosis of pancreatic cancer by 2[^{18}F]-fluoro-2-deoxy-D-glucose positron emission tomography. *Gut.* 1995;36:771–777.
16. Shreve PD. Focal fluorine-18 fluorodeoxyglucose accumulation in inflammatory pancreatic disease. *Eur J Nucl Med.* 1998;25:259–264.
17. Reske SN, Grillenberger KG, Glatting G, et al. Overexpression of glucose transporter 1 and increased FDG uptake in pancreatic carcinoma. *J Nucl Med.* 1997;38:1344–1348.
18. Jones HA, Clark RJ, Rhodes CG, Schofield JB, Krausz T, Haslett C. In vivo measurement of neutrophil activity in experimental lung inflammation. *Am J Respir Crit Care Med.* 1994;149:1635–1639.
19. Kubota R, Yamada S, Kubota K, Ishiwata K, Tamahashi N, Ido T. Intratumoral distribution of fluorine-18-fluorodeoxyglucose in vivo: high accumulation in macrophages and granulation tissues studied by microautoradiography. *J Nucl Med.* 1992;33:1972–1980.
20. Guhlmann A, Brecht-Krauss D, Suger G, et al. Chronic osteomyelitis: detection with FDG PET and correlation with histopathologic findings. *Radiology.* 1998;206:749–754.
21. Tahara T, Ichiya Y, Kuwabara Y, et al. High [^{18}F]-fluorodeoxyglucose uptake in abdominal abscesses: a PET study. *J Comput Assist Tomogr.* 1989;13:829–831.
22. Bares R, Klever P, Hauptmann S, et al. F-18 fluorodeoxyglucose PET in vivo evaluation of pancreatic glucose metabolism for detection of pancreatic cancer. *Radiology.* 1994;192:79–86.
23. Diederichs CG, Staib L, Glatting G, Beger HG, Reske SN. FDG PET: elevated plasma glucose reduces both uptake and detection rate of pancreatic malignancies. *J Nucl Med.* 1998;39:1030–1033.
24. Heinrich S, Goerres GW, Schafer M, et al. Positron emission tomography/computed tomography influences on the management of resectable pancreatic cancer and its cost-effectiveness. *Ann Surg.* 2005;242:235–243.
25. Ruf J, Lopez Hanninen E, Oettle H, et al. Detection of recurrent pancreatic cancer: comparison of FDG-PET with CT/MRI. *Pancreatology.* 2005;5:266–272.
26. Saisho H, Yamaguchi T. Diagnostic imaging for pancreatic cancer: computed tomography, magnetic resonance imaging, and positron emission tomography. *Pancreas.* 2004;28:273–278.
27. van Kouwen MC, Jansen JB, van Goor H, de Castro S, Oyen WJ, Drenth JP. FDG-PET is able to detect pancreatic carcinoma in chronic pancreatitis. *Eur J Nucl Med Mol Imaging.* 2005;32:399–404.
28. Quon A, Chang ST, Chin F, et al. Initial evaluation of ^{18}F-fluorothymidine (FLT) PET/CT scanning for primary pancreatic cancer. *Eur J Nucl Med Mol Imaging.* 2008;35:527–531.
29. Vesselle H, Grierson J, Muzi M, et al. In vivo validation of 3′deoxy-3′-[^{18}F]fluorothymidine ([^{18}F]FLT) as a proliferation imaging tracer in humans: correlation of [^{18}F]FLT uptake by positron emission tomography with Ki-67 immunohistochemistry and flow cytometry in human lung tumors. *Clin Cancer Res.* 2002;8:3315–3323.
30. Francis DL, Freeman A, Visvikis D, et al. In vivo imaging of cellular proliferation in colorectal cancer using positron emission tomography. *Gut.* 2003;52:1602–1606.

31. Buck AK, Hetzel M, Schirrmeister H, et al. Clinical relevance of imaging proliferative activity in lung nodules. *Eur J Nucl Med Mol Imaging.* 2005;32: 525–533.
32. Barthel H, Perumal M, Latigo J, et al. The uptake of 3′-deoxy-3′-[^{18}F]fluorothymidine into L5178Y tumours in vivo is dependent on thymidine kinase 1 protein levels. *Eur J Nucl Med Mol Imaging.* 2005;32:257–263.
33. Shields AF, Briston DA, Chandupatla S, et al. A simplified analysis of [^{18}F]3′-deoxy-3′-fluorothymidine metabolism and retention. *Eur J Nucl Med Mol Imaging.* 2005;32:1269–1275.
34. Perumal M, Pillai RG, Barthel H, et al. Redistribution of nucleoside transporters to the cell membrane provides a novel approach for imaging thymidylate synthase inhibition by positron emission tomography. *Cancer Res.* 2006;66:8558–8564.
35. Muzi M, Mankoff DA, Grierson JR, Wells JM, Vesselle H, Krohn KA. Kinetic modeling of 3′-deoxy-3′-fluorothymidine in somatic tumors: mathematical studies. *J Nucl Med.* 2005;46:371–380.
36. Buck AK, Bommer M, Stilgenbauer S, et al. Molecular imaging of proliferation in malignant lymphoma. *Cancer Res.* 2006;66:11055–11061.
37. Cooper LS, Gillett CE, Smith P, Fentiman IS, Barnes DM. Cell proliferation measured by MIB1 and timing of surgery for breast cancer. *Br J Cancer.* 1998;77:1502–1507.
38. Kenny LM, Vigushin DM, Al-Nahhas A, et al. Quantification of cellular proliferation in tumor and normal tissues of patients with breast cancer by [^{18}F]fluorothymidine-positron emission tomography imaging: evaluation of analytical methods. *Cancer Res.* 2005;65:10104–10112.
39. Pio BS, Park CK, Pietras R, et al. Usefulness of 3′-[F-18]fluoro-3′-deoxythymidine with positron emission tomography in predicting breast cancer response to therapy. *Mol Imaging Biol.* 2006;8:36–42.
40. Troost EG, Vogel WV, Merkx MA, et al. ^{18}F-FLT PET does not discriminate between reactive and metastatic lymph nodes in primary head and neck cancer patients. *J Nucl Med.* 2007;48:726–735.